EFDA–JET–PR(07)14

E.R Solano, S. Jachmich, F. Villone, N. Hawkes, Y. Corre, B. Alper, A. Loarte,
R.A. Pitts, K. Guenther, A. Korotkov, M. Stamp, P. Andrew, J. Conboy,
T. Bolzonella, M. Kempenaars, A. Cenedese, E. Rachlew
and JET EFDA contributors

ELMs and Strike Point Movements

ELMs and Strike Point Movements

E.R Solano[1], S. Jachmich[2], F. Villone[3], N. Hawkes[4], Y. Corre[5], B. Alper[4], A. Loarte[6], R.A. Pitts[7], K. Guenther[4], A. Korotkov[4], M. Stamp[4], P. Andrew[4], J. Conboy[4], T. Bolzonella[8], M. Kempenaars[9], A. Cenedese[10], E. Rachlew[11]
and JET EFDA contributors*

[1]Asociación Euratom/CIEMAT para Fusión, Madrid, Spain
[2]ERM/KMS-LPP, Association EURATOM-Belgian State, Brussels, Belgium
[3]Universitá di Cassino, Association EURATOM/ENEA/CREATE, DAEIMI, Cassino, Italy
[4]EURATOM-UKAEA Fusion Association, Culham Science Centre, Abingdon, U.K.
[5]Euratom-CEA Association, CEA-Cadarache, 13108, St Paul lez Durance, France.
[6]EFDA Close Support Unit, MPI fur Plasmaphysik, Garching, Germany
[7]CRPP, Ass. EURATOM-Confédération Suisse, EPFL, 1015 Lausanne, Switzerland.
[8]Consorzio RFX, Associazione Euratom-ENEA sulla Fusione, Padova, Italy
[9]FOM-Rijnhuizen, Ass. Euratom-FOM, TEC, PO Box 1207, 3430 BE Nieuwegein, NL
[10]D.I.E., Università di Padova, Via Gradenigo 6/A, I-35131 Padova, Italy
[11] Euratom-VR Association, Dept of Physics, KTH, 10691 Stockholm, Sweden
** See annex of M.L. Watkins et al, "Overview of JET Results ",*
(Proc. 21 st IAEA Fusion Energy Conference, Chengdu, China (2006)).

Preprint of Paper to be submitted for publication in
Nuclear Fusion

ABSTRACT.
A detailed study of position changes of plasma strike points before and after ELMs in JET was carried out. A hypothesis being tested is that in an ELM previously closed edge field lines would open up, releasing plasma current and leading to the formation of a new, smaller separatrix. It was observed that after each ELM strike points have shifted a few cm towards the plasma centre (up in JET). In some cases a transient (<100 microseconds), upwards large (>10cm) jump of strike positions was observed first. It was followed by an equally fast jump down to the shifted strike positions. Such behaviour has not been described in previous computational models of the ELM. Therefore two novel instability mechanisms are presented, which contribute to explain the changes in strike point position: an X-point instability, due to positive toroidal current density at the X-point, and a diamagnetic instability, due to negative inboard toroidal current density.

1. INTRODUCTION

Theoretical studies of equilibrium criticality [1] inspired an experimental study of changes in plasma equilibrium before and after ELMs. In that theoretical work it was conjectured that an ELM could be due to local loss of plasma equilibrium from a critical point out to the last closed flux surface. Some of the previously closed flux surfaces near the plasma edge would open, leading to fast loss of particles, energy and current along the newly opened field lines. One might say the plasma edge peeled away. A new equilibrium would be formed, with a smaller separatrix. Expected observable consequences of the peeling off of previously closed flux surfaces in a diverted plasma would be a sudden change in strike point positions and sudden loss of plasma current at the ELM. In this study we investigate the shedding of previously closed flux surfaces as an ELM model.

Regardless of the origin of the prediction, peeling of previously closed flux surfaces could be due to equilibrium criticality [1], and/or to complex evolution of initial ballooning, peeling or peeling-ballooning instabilities [2 ,3, 4, 5]. These later MHD models of the ELM, much discussed of late, do not consider the possible shedding of previously closed flux surfaces, as typically the plasma boundary is held fixed throughout the computational simulation of such instabilities.

Designing the experiment, it was considered desirable to study large, infrequent ELMs. The absolute change in total stored energy before and after the ELM is used as a measurement of ELM size. Such ELMs were expected to produce more easily observable strike point changes. It was important to use many core and edge simultaneous measurements to facilitate the pre-ELM equilibrium reconstruction. A plasma shape was designed with optimum diagnostic access for edge diagnostics (Langmuir probes, infrared camera, edge profiles).

Interestingly, large infrequent ELMs in JET are most easily obtained in natural density pulses (with no gas-puff). This leads to a particularly ITER relevant hot plasma edge: the electron temperature (T_e) at the top of the pedestal is typically 1.5keV, to be compared with an expected pedestal T_e ~ 3-4keV in ITER. With such high electron temperature the plasma resistivity is low and substantial toroidal and poloidal edge current densities can be present. It is found that this has important

consequences on pre-ELM equilibria, in agreement with an earlier study in DIII-D [6].

This paper is organised as follows: in section 2, a description of the reconstructed pre-ELM equilibrium situation is presented, together with comments on the expected consequences of edge plasma peeling in that type of equilibrium; in section 3 experimental observations of plasma strike movements are presented and discussed; in section 4 numerical modelling of plasma peeling is presented; in section 5 two novel potential ELM triggers are described; in section 6 equilibrium criticality is discussed; in section 7 we bring the various elements of the study together to show that our peeling model of the ELM provides a good overall explanation of the observed plasma behaviour, and consider alternate models. Finally conclusions are presented in section 8.

Theoretical background: plasma equilibrium before the ELM, and plasma peeling

Plasma force balance in a magnetic confinement device with closed field lines is given by the equation:

$$\mathbf{j} \times \mathbf{B} = \nabla \mathbf{p} \tag{1}$$

in which j is the total current density, B the magnetic field and p the pressure. On closed flux surfaces the pressure is usually a monotonic function of Ψ, the poloidal magnetic flux per radian, $p=p(\Psi)$. Therefore the pressure gradient can be represented as $\nabla p = (dp/d\Psi)\nabla Y = p'\nabla Y$. The prime indicates the derivative with respect to Ψ.

Assuming nested flux surfaces and toroidal symmetry, equation (1) leads to the Grad-Shafranov equation [7] as a description of plasma equilibrium in a tokamak:

$$\frac{1}{\mu_0 R}\left(R\,\frac{\partial}{\partial R}\frac{1}{R}\frac{\partial \Psi}{\partial R}+\frac{\partial^2 \Psi}{\partial Z^2}\right)+\left(R\,p'+\frac{(F^2)'}{2\mu_0 R}\right)=0 \tag{2}$$

In (2) the first term is a linear operator acting on Ψ, $L(\Psi)$. The second parenthesis is the toroidal current density,

$$j_{toroidal} = Rp'(\Psi) + FF'/(\mu_0 R) \tag{3}$$

which can be considered as a non-linear operator, J, acting on Ψ via the Ψ dependency of p' and FF'. (R,Z,ζ) are cylindrical coordinates; Y is measured outwards from the plasma magnetic axis; F is the toroidal magnetic field flux function.

Equilibrium reconstruction of the pre-ELM state is heavily influenced by how the large outboard pressure gradient, usually observed in well developed H-mode plasmas with type I ELMs, is represented.

A large pressure gradient can be associated either with a large $p'=dp/d\Psi$, or with large ∇Y. The choice is typically determined by internal magnetic or kinetic constraints. In JET ELMy H-modes, typically p' is non-zero at the outer equator across the separatrix.

As a consequence of the large edge ∇p and p', the poloidal current density is locally diamagnetic and F' has opposite sign to p' in equation (3). In a sufficiently diamagnetic edge plasma, the inboard edge toroidal current density can be negative since the F' contribution to the toroidal current density is

amplified by *1/R*, while *p'* is multiplied by *R*. This is a typical feature of H-mode plasmas [6].

As a further consequence, the toroidal current density is not necessarily zero at the X-point, unless the two terms in equation (3) happen to cancel precisely at the X-point (an unlikely coincidence, as *p* and *F* are flux functions, but *R* is an independent variable). We will return to this point in section 5, as it can lead to instability.

Internal magnetic field measurements from polarimetry and Motional Stark Effect (MSE), together with external magnetic measurements, have been used at JET to reconstruct a pre-ELM equilibrium, corresponding to the ELM event described in section 2. Its current density profiles inside the last closed flux surface are illustrated in figure 1, plotted at the plasma equator. Edge diamagnetism (negative *FF'*) is a robust feature of the reconstruction, while negative inboard $j_{toroidal}$ is not always found as reconstruction code parameters are varied, probably due to insufficient diagnostic constraints on the plasma inboard.

If local equilibrium is lost somewhere inside the separatrix, that flux surface might "break", and the previously closed flux surfaces outside it would open. Particles, energy and current would flow along these newly opened field lines and be rapidly lost. We describe such a process as a peeling of previously closed flux surfaces. The sudden loss of current (of both signs) from inside the separatrix leads to the formation of a new, smaller separatrix, with displaced X and strike points (since the divertor and shape control coil currents cannot change on the ELM timescale). The strike points would move towards the plasma magnetic axis. In plasmas with strike points arriving at horizontal target plates, the inner strike would move inward and the outer outward while with strike point incidence on vertical targets, both strike points would move upwards.

Additionally, at the inboard plasma equator, the loss of counter-current would lead to an increase in the magnitude of the local vertical field. Outboard, the magnitude of the local vertical field would decrease, as positive co-current is lost. Changes in local magnetic measurements at ELMs with this behaviour have been reported in ASDEX [8]. At the time they were first explained as an inboard plasma displacement, due to a drop in poloidal beta (β_{pol}). They are also seen in JET, as shown in figure 2. In JET the sudden changes are consistent with peeling of edge flux surfacesl, considering the inboard edge counter current: the current centroid is horizontally displaced inward at an ELM because of loss of counter current on the plasma inboard and loss of co-current on the plasma outboard, while there is no evidence from core diagnostics of a core plasma movement.

Equally, the up-down asymmetric current distribution in single null plasmas can produce apparent vertical displacements of the plasma current centroid associated with plasma peeling. These apparent displacements are observed at JET, but we can establish that the core plasma does not move. Therefore, the plasma current centroid should not be used as a control variable for plasma position in the presence of large ELMs.

Incidentally, as illustrated in figure 2, at the L to H transition the poloidal magnetic field is reduced inboard and increased outboard (see Figure 1), possibly implying that the H-mode is associated with edge diamagnetism, which reduces current inboard and increases it outboard.

Regarding localisation: peeling of previously closed can occur in ribbons or in layers. Peeling in ribbons would be more likely if there is a nearby resonant q surface and an MHD precursor. A ribbon would produce poloidally and toroidally localised power deposition. Peeling of a whole layer may occur in the absence of MHD precursors, or when a toroidally symmetric instability occurs near the X-point (see section 5).

Evidence of localised ELM effects was found in an independent study, where ELM-associated current flow outside the plasma was detected with the JET saddle coil system [9]. The saddle coils are in-vessel metallic structures, inboard and outboard, and can be directly affected by the plasma at locations about 0.5 m above the strike points. These measurements tell us that not all the plasma current loss occurs at the divertor plates, while supporting the hypothesis that plasma current is lost from the plasma at an ELM. Equally, in JET there is evidence of ELM-induced radial propagation of hot plasma across flux surfaces near the outer equator [10] and at the plasma top [11,12]. Unfortunately, none of these measurements were available for the pulses discussed here, and the measurements reported typically correspond to fairly frequent, small ELMs in relatively cold plasmas.
Other studies of ELM-associated plasma current detection in the SOL in DIII-D are described in [13, 14] and references therein. In Ref. [13] the ELM is first described as a toroidally localised event. There it was assumed that power from the main plasma is deposited in an already open field line, and then flows to the divertor target. More complex non-axisymmetric energy deposition patterns were observed in AUG [15], and interpreted as footprints of approximately field aligned, helical perturbations of a SOL flux tube loaded by plasma expelled from the pedestal region. Fluctuation studies in AUG and JET also show that localised blobs exist in the SOL during ELMs [16], and it is proposed that these blobs carry the plasma energy across the separatrix and out of the plasma. Observations in MAST also emphasize the localised nature of ELMs, beautifully captured in fast video images [17, 18], and analysed with many diagnostics. In this last case, the data is discussed in terms of “plasma filaments”: SOL flux tubes loaded by enhanced heat conduction from a closed field line that balloons out from the pedestal region at the outer equator.

Plasma peeling in ribbons, separatrix break-up and formation of a smaller separatrix can account for several of the observed features described in the above references. Importantly, loss of edge current is an inescapable result of the sudden loss of plasma particles in the ELM, which has not so far been considered when modelling experimental observations. We consider it possible that in some cases plasma peels in ribbons (leading to apparent plasma filaments, but not-necessarily driven by a ballooning mode), while in other cases peeling occurs in layers, leading to a toroidally symmetric ELM footprint. In this study in JET we lack the toroidal coverage necessary to ascertain which ELMs peel off as ribbons and which as layers, so both possibilities remain. However the transitional loss occurs, the pre and post ELM states are considered to be toroidally symmetric.

3. TYPE I ELMS IN JET: EVIDENCE OF STRIKE POINT MOVEMENTS.

ELM-induced strike point sudden shifts in JET plasmas were first reported in 1995 [19, 20]. The

observation of a sudden inward shift of the inner strike and an outward shift of the outer one was made jointly with an infrared camera, soft X-ray arrays and Langmuir probe arrays.

More recently, specific experiments have been designed and executed to investigate the pre-ELM equilibrium and subsequent strike point movement during ELMs in JET [21, 22], and to contrast the simultaneous observations of various diagnostics. To maximize diagnostic sensitivity, plasmas were designed with infrequent large ELMs and strike point positions were optimised for good InfraRed (IR) viewing and divertor target Langmuir Probe (LP) array coverage. Discharges yielding the best data had 2.4MA of plasma current, toroidal field of 2.4T, 15MW of neutral beam injection heating and low or no gas-puff during the heating phase. Pedestal densities varied from 3.10^{19} to 7.10^{19} m^{-3} (raising in between ELMs), while pedestal electron temperatures were in the range 1-2keV. These plasmas are characterised by 1Hz compound ELMs. Compound ELMs [23] are often observed in JET at low densities: they exhibit a large initial D_α spike, followed by a short period of lower D_α spikes, often considered as a Type I ELM followed by a string of Type III ELMs. Sudden energy loss occurs in the "Type I" phase of the compound ELM, with further slow losses during the "Type III" phase. In the experiments reported here the sudden drop in diamagnetic energy is of order ΔW_{dia}= 0.5MJ, within the first 100 ms or less (indicated by SXR measurements), followed by a subsequent energy drop of order 0.5 to 1MJ, in 100-200ms. There is no back-transition to L-mode.

Figures 3 and 4 illustrate typical observations of strike point movements at a compound ELM in JET. The contour plots of tile surface temperature (figures 3b, 4b) and ion saturation current (figures. 3c, 4c) clearly show both the pre-ELM position and how subsequent small ELMs arrive at a higher location, about 2 cm above the pre-ELM location. The strike points have shifted after the leading fast transient event. Later, after the end of the ELM phase, the strike points return towards the pre-ELM position. On a faster time scale, at the diagnostic time resolution limit, much larger strike jumps are often observed, associated with the leading ELM of the compound ELM. Note in figure 3d and 4d that the LP array detects sudden large strike point position jumps, about 20 cm inboard and 7 cm outboard (see also figure 5). The inboard observation of the sudden jump is supported in part by the IR diagnostic, in the form of a bright flash visible 12 cm above the pre-ELM position inboard. This transient surface heating disappears in less than 65μs (Fig 3b). The IR response to such transients is enhanced at the inboard tiles by the presence of a thin layer of co-deposited material with poor thermal conductivity, which reacts quickly to the incoming ELM power. On the outboard tiles, the IR contours in figure 3b show a new strike position (temperature rises at a point higher than the pre-ELM strike position), but the pre-ELM strike position remains hot for some time even after power ceases to arrive at it (there are no deposited and the thermal response is slower). Since in figure 4d the position of the hottest pixel is shown, it appears that the "strike movement" occurs later. In fact, what is shown is that only at 21.5 s has the outer pre-ELM strike position cooled down sufficiently for the hottest pixel to be at the new strike position.

Some details on Langmuir probe measurements are presented in figure 5. Figure 5a illustrates the time evolution of ion saturation current profiles in the outboard LP array for the front of the ELM

depicted in figures 3 and 4, during only the first 500μs (before the full rise of the first D_α spike of figure 3). The black curve (at 21.4071 s) is the pre-ELM profile, the red curve (at 21.4072s) corresponds to the high strike point observation (the strike jump), and the blue curve, (21.476s), shows the settled strike position (the strike shift).

In figure 5b we show an ELM from a different pulse. Here the data is easily described as a transient strike jump from -1.65m to -1.55m, and a subsequent shift of strike position to ~-1.63m. As a shorthand, we shall describe these changes in the deposition of ion saturation current as strike jumps when the maximum moves to a new probe for only one time point (100μs), and as a shift when the strike remains at a new post-ELM position for considerable time (milliseconds or more).

It is important to emphasize that the strike jumps and shifts shown are difficult to interpret as "plasma filaments" being detected by the LPs at the ELM: if that was the case, there would be at least 2 clear peaks, one associated with the filament, another associated with the strike point of the bulk plasma. On the other hand, the secondary peak shown at -1.4 m in figure 5a could be due to such a filament, albeit long lived. It could also be considered as a stripe, similar to the stripes reported from infrared measurements in AUG [15,24]. As such stripes are not always present or detected with our LPs or IR systems, we shall not analyse them further. They do not play a dominant role in our study.

Are upward strike jumps and shifts due to global plasma movements? We know they are not in this case. The vertical position of the centre of SXR emission (central channels only) has a downward dip and recovery of 2mm in 160μs (probably due to edge surfaces in the line of sight), and in a longer time scale it shows a slow upward drift. The initial small downward movement of the plasma centre cannot explain an upward multi-cm displacement of the strike points.

It is also interesting to point out that the signal from the SXR channel just inside of the X-point (diagonal line from outer equator towards the divertor region) shows a decrease in signal amplitude about 20μs before the top SXR channel signal decreases, as shown in figure 6a and 6b. In 6c and 6d we show a magnetic coil signal and the inner D_α, to show that this is the very beginning of this ELM. These SXR signals can be interpreted as an indication that the plasma loss begins at the X-point. To qualify such conclusion: first, many but not all of the large ELMs we have analysed show plasma loss near the X-point to precede the top or equator plasma loss, second, as all the relevant SXR channels are at the same toroidal cross-section, toroidal asymmetry could play a role in the interpretation of SXR data. Plasma loss could occur first at the outer equator, as a detachment of a bundle of flux tubes peeled from the plasma. It might be seen as a sudden loss at a different poloidal location (such as the X-point), depending on plasma rotation and the toroidal cross section where the diagnostic is placed. A more careful statistical study of SXR evolution would be required to discard this alternate explanation.

Additional evidence of plasma edge erosion, rather than global plasma movement, comes from edge density measurements, obtained with a Li beam along a vertical line at the plasma top (100μs time resolution). After each ELM, loss of density is observed from the top edge surfaces, as shown in figure 7. In the top plot it is shown that the edge density falls after each of the 3 ELMs. Complementarily, the line integrated density is measured along 3 interferometre vertical lines located inboard and outboard

of the magnetic axis and at the outer edge (up to 1 ms time resolution). The drop of the line integrated density of all interferometer line integrals in the time scale of the compound ELM indicates that the density loss observed by the Li beam is not due to an in-out movement of the plasma centre. On a faster time scale (<1 ms), the simultaneous drop of the edge line and rise in the core lines is harder to interpret, as the core lines intersect the SOL in the divertor region, responding to the arrival of plasma from other regions, presumably now along open field lines.

Finally, evidence of ELM power deposition away from the pre-ELM strike positions is found in thermocouple measurements from the plasma divertor tiles. The ThermoCouples (TCs) are embedded 1cm deep in the divertor tiles. There are TCs at –1.64m, the height of the inter-ELM strike point position, and 10cm higher. Typically, the inter-ELM SOL width is ~1-3 target cm, so little heat arrives directly at the upper TCs in between ELMs. During the ELMing phase of the discharge, the bulk of the Temperature (T) rise is near the lower TCs, as shown in Fig 8 (red traces in top row). Small and clearly visible heat pulses associated with ELMs are observed on the T and dT/dt traces, particularly in the lower TC of the inner tile and the upper TC of the outer tile. These measurements show that ELMs deposit considerable heat away from the pre ELM strike position. During this pulse 46.5MJ (60% of total energy input) are deposited in the outer lower tile, and 15MJ (20%) in the inner tile. Figure 8 shows that in the inner tile ELM heat pulses are deposited near both lower and upper TCs, approximately at the same time (dT/dt signals are in phase). In the outer divertor tile ELM heat pulses arrive in phase with ELMs at the upper TC, out of phase at the lower TC. This implies that arrival of ELM heat pulses at the lower TC must be indirect: heat is deposited elsewhere and conducted to the TC, or arrive later, when the strike point has returned to the pre-ELM position. These measurements are also compatible with our model of the ELM as a peeling of previously closed flux surfaces, leading to energy deposition above the pre-ELM strike positions.

4. MODELLING PLASMA PEELING

Starting from the equilibrium depicted in figure 1, a linearised plasma response model [25] is used to compute a new equilibrium by peeling surfaces outside a given normalised Y value, accounting for induced currents in passive structures (large in sudden events in JET). The eddy currents can be considered, in part, as a representation of the currents flowing in the Scrape-Off Layer (SOL), which transiently oppose the initial flux changes. Peeling flux surfaces outside of $\Psi_N = 0.97$ results in the loss of 46kA of toroidal current, a loss of plasma diamagnetic energy ΔW_{dia}~0.5MJ, and upward strike shifts of 4cm inboard, 3cm outboard.

A breakdown of the various contributions to the total system energy before and after the ELM is presented in Table 1. It is interesting that due to the loss of diamagnetic current from the plasma edge, the largest changes are an exchange of the toroidal field energies in plasma and vacuum regions. The drop in kinetic pressure and poloidal field energy is compensated in part by the increase in toroidal plasma field energy inside the plasma, larger than the decrease of toroidal field energy outside the plasma. The final state has a 0.4MJ drop in plasma kinetic energy, approximately consistent with the

experimental observation of ΔW_{dia}. As the peeled state has lower energy than the pre-ELM state, peeling of flux surfaces is a physically allowable transition between neighbouring equilibria.

The pre and post-ELM strike positions of the reconstructed equilibrium are compared with LP measurements in Table 2. They show good agreement with LP measurements outboard (where more measurement constraints are available), but not inboard. Alternative reconstructed equilibria, adding edge pressure constraints, can strongly reduce the discrepancy in the pre-ELM inboard strike position, but choosing amongst the various alternatives is non-trivial. For now, we present the results of the initial reconstruction simply to gauge the effects of peeling, while admitting that model results may depend strongly on equilibrium reconstruction details of the pre- ELM state that cannot (yet) be ascertained.

One possible explanation for the large sudden jumps is that they are associated with the non-zero toroidal current density at the X-point. As the separatrix breaks, the X-point co-current carrying flux tube is displaced towards the private flux region [26]. There it will be accelerated further towards the divertor coils since the attractive j×B force from the core plasma decreases while the force from the divertor coils increases. Transiently, a new X-point would form, closer to the core plasma, when the externally imposed diverting fields are increased by the field produced from the detached current carrying flux tube. This situation has been modelled by adding the toroidal lost plasma current, 40 kA, to the divertor coils, to simulate the presence of currents flowing transiently in the SOL, including the private flux region. Again, results of these model equilibria are shown in the first 2 rows of Table 2 next to LP measurements, and agreement is fairly good for outboard strike movements.

In the private flux region the connection length is 5m, so current flowing along open field lines would arrive at the target plates and be lost in about 10μs (assuming 1.5 keV ions to compute sound speed). In the main SOL the connection lengths from the midplane are 20m, so those SOL currents would disappear in 50ms, or faster if current filaments are displaced radially sufficiently fast. The post-ELM state would therefore be reached in 50ms or less. This is consistent with the fact that the sudden large strike jumps are only seen in 1 time point of the 10 kHz LP data [21], and only occasionally with the IR camera (1 frame = 3ms).

5. INSTABILITIES DRIVEN BY EDGE CURRENTS

The toroidal current at the X-point (discussed above) might itself trigger the ELM. If the toroidal current density increases in magnitude as the X-point is approached from the plasma core, a position instability of the current carrying X-point flux tube could be responsible for breaking of the separatrix. A simple magneto-static model of this X-point instability is presented in [26], simulating a double null plasma with straight current filaments. The evolving pre-ELM state can be described by displacing 2 current filaments (each carrying 2% of the total plasma current) towards the X-points, from the plasma centre. Results are presented in the bottom row of Table 2. As the filaments are swept towards the divertor coils, but still inside the main separatrix, the strikes sweep down to –1.66m. In the transient state, while current flows in the private flux regions, up to 6†cm upward strike jumps can be explained. For a given plasma configuration, increasing

$\beta_{poloidal}$ and triangularity increases diamagnetism and reduces the toroidal current density at the X-point, increasing the positional stability of the current-carrying X-point. Equally, higher edge densities lead to colder edges, with less current. Both of these circumstances would reduce the drive for X-point current instability. Type II ELM behaviour, usually associated with high triangularity and high density (cold edge), could be associated with more stable X-points [27].

Besides affecting the stability of a current carrying X-point, diamagnetism may itself provide an alternate instability mechanism contributing to the ELM trigger. As described in Section 1, as the pressure gradient increases, diamagnetism drives the inboard $j_{toroidal}$ more negative, while the outboard $j_{toroidal}$ increases with the increase in p'. The repulsion between regions with opposing current density (poloidal and toroidal) might render the equilibrium fragile on the high field side. Measurements of poloidal magnetic field (figure 2) at the inboard and outboard plasma equator are consistent with the growth of counter $j_{toroidal}$ inboard and co-current outboard before the ELMs, and the loss of such edge currents after the ELM. In an independent study it was found that on average the inboard magnetic probes detect the ELM crash 30μms earlier than the outboard probes [10].

6. EQUILIBRIUM CRITICALITY ANALYSIS

Considering equation (2) as a non-linear partial differential equation, we can study its criticality [1]: the identification of situations such that the number of solutions of the equation changes under a small perturbation of the equation. As shown in [1], criticality of the Grad-Shafranov equation can be tested in the neighbourhood of a solution $\Psi(R,Z)$ by searching for regions of the plasma where the operator equation

$$\partial J/\partial \Psi = J/\Psi \tag{4}$$

is locally satisfied. Here J is the toroidal current density (a function of R and Ψ), and Ψ is the poloidal magnetic flux measured from the plasma magnetic axis. The condition was derived setting the part of the equation linear in Ψ to zero: non-linear equations with zero slope are critical.

That theoretical study led us to conjecture that the formation of a transport barrier corresponds to the appearance of a new solution branch of equation (2) with a locally diamagnetic region. The equilibrium reconstruction presented in figure1 does display diamagnetism in the edge barrier region, in agreement with this conjecture. Evidence for a possible association between diamagnetism and the L-H transition can be seen in figure 2b, where we show the local poloidal magnetic field inboard and outboard of the plasma, at the plasma equator. Clearly there is a break in the time derivative at the L to H transition, as would be expected if diamagnetism increased at this point.

Conversely, we conjecture that in critical situations, a given equilibrium may be locally fragile. From there the plasma could peel off, be it in ribbons or as a complete layer. Note that equilibrium fragility is different from MHD stability of a given plasma state: we make no statement about the

dynamics of the plasma evolution. Having said that, as condition (4) acts on the current density profile, criticality is likely to be associated with current driven instabilities, diamagnetism and tearing modes.

An ELM could be the consequence of equilibrium fragility, a local loss of solution. The particular equilibrium depicted in figure 1 does not satisfy the criticality condition (4) at the equatorial edges or the X-point: this equilibrium is not fragile. Minor modifications of the edge current profiles can produce nearby equilibria that satisfy the criticality condition. In particular the addition of pre-ELM edge pressure measurements from Thomson scattering near the X-point does lead to an equilibrium that is fragile at $\Psi_N = 0.95$ near the X-point. Regrettably, given our present equilibrium reconstruction capabilities we can say that equilibrium fragility at the X-point, inboard or outboard equator are all possible situations before an ELM, but stronger statements cannot be made at the moment.

7. DISCUSSION AND COMPARISON WITH OTHER ELM STUDIES

Plasmas with low density were chosen for this study for diagnostic reasons, as the ELMs in such plasmas are rather infrequent, allowing for optimum use of the diagnostics with low time resolution, which are useful for detailed equilibrium reconstruction. The low edge density implies that the edge temperatures are high, and therefore these plasmas have both low edge resistivity and collisionality:

Typical electron temperatures at the top of the pedestal in our experiments are 1.5keV, with associated resistivity $\eta \sim 1.35\ 10^{-8}\ \Omega$-m. For reference, the pedestal e-e collisionality is $\nu_{ped}^* \sim .07$. Colder plasma edges, studied in JET and other tokamaks, have pedestal electron temperatures of order 200eV, and resistivity is 20 times higher. Therefore hot edge plasmas can have large edge currents, poloidal and toroidal. This implies that current-driven instabilities are more likely to be dominant in these plasmas. Also, the measured pressure gradients before these large ELMs are largest at the lowest plasma densities [28], and ballooning modes could be unstable as well. Here we must point out that from the point of view of MHD instabilities driven by edge current density, the ITER relevant situations correspond to hot plasma edges ($T_{e,ped}$ in ITER is expected to be 3.-4keV [29), with low resistivity and large current density, such as the ones studied here.

Studies of ELM precursors in JET [30, 31] show that precursor oscillations do not grow exponentially into the ELM crash but mostly rather linearly, or not at all, sometimes even disappearing altogether before the ELM crash [32]. Such ideal modes are therefore not ELM triggers. For instance, in the case of the ELM shown in figure 3, an edge oscillation (an “outer” or “peeling” mode with n = 7, 10kHz) is created immediately after a sawtooth crash (8ms before the ELM), its amplitude is steady, and it is terminated by the ELM.

Rather than to ideal instabilities, type I ELMs appear to be more closely related to fast crash events, like sawteeth and disruptions, as discussed in [33]. Characteristic times for the ELM crash peeling transition at the X-point can be estimated with the Kadomtsev sawtooth model [34]. The local AlfvÈn time would be associated with the change in poloidal field at the X-point, $\delta B_{pol} \sim 5\ 10^{-2}$ T (using our estimate of how much the poloidal field changes near the X-point due to

peeling of flux surfaces), the displacement of the X-point due to peeling, $\delta r \sim 5$ cm, the local density $n_i \sim 1\text{-}5\times10^{19}$, and temperatures $T_e \sim$ 50-500 eV: $\tau_A = \delta r\,(\mu_0\, n_{ion}\, m_{ion})^{1/2}/\delta B \sim$ 0.2-0.5μs. The resistive time is $\tau_R = m_0\,(\mu r)^2/\eta \sim$ 1-33ms. The Kadomtsev time would be $\tau_K = (\tau_A \tau_R)^{1/2} \sim$ 10-100μs. This time scale is a better match to the ELM crash time than the zero growth rate of precursor modes. A similar time scale would be associated with the diamagnetic instability due to the negative inboard current, proposed in Section 3.

The most widely accepted model of type I ELMs, the peeling-ballooning mode, is described in recent reviews [4,5] and references therein. Various numerical codes are used to calculate the MHD stability of the plasma before an ELM, and there is apparent good agreement between calculations of pedestal stability and the appearance of ideal MHD modes. On the other hand, it must be noted that in most simulations the last closed flux surface is held as a fixed boundary, it contains no X-points and carries no current. Even in ref. 4, where an X-point and finite resistivity are included, it is not possible to model X-point instabilities, since the current at the separatrix is set to zero. So the modelling does not produce strike point movements, and can not test our proposed instability mechanisms associated with current density at the X-point, or negative toroidal current at plasma inboard. Further, cartoons presented, for instance, in figure 6 of reference [5] do not reflect what is measured at JET in these pulses, as the flux surfaces are represented as stationary.

It has also been proposed that the ELM may be due to an X-point interchange stability between the cold SOL and the hot edge plasma [35]. This could be related to the proposed X-point instability, but a direct comparison with that model is not possible, as realistic geometry and profiles would need to be added to it, a non-trivial exercise. Based on ELM experimental studies at JET, Gill [30] also proposed that plasma from inside the separatrix is exchanged by the ELM instability into a layer outside the separatrix which then flows down into the divertor region or onto a limiter. The evidence presented in that article would be equally compatible with plasma peeling as we propose here.

Let us turn now to a qualitative discussion of the apparent strike jumps and stripes. Common interpretations of the data shown in figure 3 are that power deposition away from the pre-ELM strike position is due to SOL hot filaments arriving at the strike plates [17], or due to ergodization of the separatrix [36]. Such considerations would not explain the consistent strike shifts we observe at ELMs, since ELM filaments or ergodic field lines would arrive both above and below pre-ELM strike locations. They might provide explanations for the occasionally observed stripe formation shown in figure 5a, or contribute to the explanation of the strike jumps observed in JET. If the pre-ELM separatrix breaks, SOL field lines that used to arrive just above the pre-ELM strike point positions will move. If a new separatrix forms quickly and robustly (as we attempted to model in Section 3), the SOL field lines would be pushed upwards transiently, above the new strike points. But before this new separatrix is formed, the previously closed field lines could be ripped from the plasma core, possibly in ribbons or layers, and we might be detecting the intersection of these hot ribbons or layers with our diagnostic views in our apparent strike jumps and/or stripes. They would all appear above the pre-ELM strike positions. If, on the other hand, complete ergodisation occurs before the new separatrix forms, the

SOL footprint would broaden around the pre-ELM strike positions, both upwards and downwards, which is not consistent with our observations. An intermediate situation between toroidally symmetric strike jumps and separatrix ergodisation may be present if homoclinic tangles [37] have time to form, and remain stable: stripe patterns would form. Ergodisation and homoclinic tangles are more likely to occur in dense, cold edge plasmas, as high resistivity facilitates small scale topological changes. A related possibility, which also results in the formation of stripe patterns, is described in [15]: during the ELM localised bursts of particles and energy would load a SOL flux bundle. Particles and energy would flow along the field lines and intersect the target along stripes near the pre-ELM strike point. The secondary outboard stripe shown in figure 5a could be produced by various combinations of the above-mentioned "hot filament" models, but it is not possible to ascertain the underlying cause for the apparent strike jumps.

Yet another family of ELM models is often discussed: an explosively growing ballooning mode [38]. The fast energy loss at an ELM would be due to diffusion from the pedestal into the SOL, enhanced by the locally large pressure gradient in front of the twisting hot plasma flux tube that pushes its way out towards the last closed flux surface at the outer equator. The transported power and particles would flow along the SOL field lines to the pre-ELM outer strike position, or elsewhere if this model is combined with any of the models above mentioned. In [39] it is shown that images of plasma "fingers" observed in MAST match the topology of a computed field line mode. Other computational simulations of the non-linear evolution of mixed peeling-ballooning modes [2] show plasma filaments reaching across the separatrix at the outer equator. In considering the relevance of this model to explain our observations, we find that non-linearly growing peeling-ballooning modes are more typically present in experiments and simulations with relatively high edge density and low edge temperature, implying low plasma current density. In low resistivity edges, like ours, data analysis and simulation show that the first unstable modes have a low n kink character, and are localised at the X-point [see Ref.31, figs. 15 and 17]. In consequence, plasma filaments might reach the target from the X-point region, rather than from the outer equator, and they may not be due to ballooning modes. Independently of their formation mechanism and dynamics, if plasma filaments reach across the pre-ELM separatrix, they would carry current away from the plasma, as well as particles and energy. This would lead eventually to a new equilibrium with a smaller separatrix and displaced strike points, as we observe in JET for large enough ELMs.

There are control issues associated with our observations: if ELMs in plasmas with hot edges are due to a loss of previously closed flux surfaces, the current centroid becomes a non-optimal measurement of plasma position, as loss of X-point current may appear to be an upward displacement of the plasma, deceiving the control system into attempting to oppose it.

CONCLUSIONS

The study of strike point positions in JET, before and after ELMs, complements other profile and magnetic information. The experimental data clearly shows that strike points are shifted upward a few

cm soon after an ELM event (about 100μs after the D_α rise). During a fast transient phase, the dynamic evolution is more complex, larger upward displacements can be observed, up to 20cm.

We have explored the possibility that ELMs are associated with a breaking of previously closed flux surfaces, including the separatrix. The experimental evidence does support such a "peeling" model of type I ELMs. During the transient phase, an overshoot of the strike shifts could be due (in part) to the presence of toroidal currents in the private flux region, transiently driving the strike points further up, although a variety of other interpretations is possible.

Two novel instability mechanisms were considered, both associated with edge currents: the X-point instability and the diamagnetic instability. Details of the pre-ELM equilibrium reconstruction are still insufficiently quantified for reliable equilibrium criticality or MHD stability studies in this case.

Regardless of which instability mechanism triggers the ELM, the evidence for eventual peeling of a plasma layer, homogenously or in ribbons, remains. Therefore a more complete model of the ELM for transport and edge models should take into account the new flux surface geometry, with a reduced separatrix.

ACKNOWLEDGEMENTS:

We would like to acknowledge useful discussions with Roberta Sartori, Gabriella Saibene, Guido Huysmans, Steve Cowley, Tod Evans and Phil†Snyder. This work has been conducted under the European Fusion Development Agreement, and has been funded in part by a Ramón y Cajal grant from the Ministerio de Educación y Ciencia, Spain.

REFERENCES

[1]. Solano E.R, 2004 *Plasma Phys. Control. Fusion* **46**, L7

[2]. Connor J.W, Hastie R.J, Wilson H.R and Miller R.L, 1998 Phys. Plasmas **5**, 2687-2700

[3]. Snyder P.B, Wilson H.R, Xu X.Q, 2005 *Phys. Plasmas* **12** 056115

[4]. Huysmans G.T.A, 2005 *Plasma Phys. Control. Fusion* **47**, B165-B178

[5]. Wilson H.R, Cowley S.R, Kirk A, Snyder P.B, 2006 *Plasma Phys. Control. Fusion* **48** A71-A84

[6]. Lao L.L, 1990 *Nuclear Fusion* **30** 1035

[7]. Grad H, Rubin H 1958 "MHD Equilibrium in an Axisymmetric Toroid". *Proceedings of the 2nd UN Conf. on the Peaceful Uses of Atomic Energy* **31**, Vienna, IAEA, p.190; Shafranov V D 1966 "Plasma equilibrium in a magnetic field", *Reviews of Plasma Physics* **2**, New York: Consultants Bureau, p. 103.

[8]. Von Goeler S, Kluber O, Fussmann G, Gernhardt J, Kornherr M 1990 *Nuclear Fusion* **30** 395

[9]. Testa D, Bigi M, 2005 *Plasma Phys. Control. Fusion* **47** 733.

[10]. Fundamenski W, Sailer W and JET EFDA Contributors, 2004 *Plasma Phys. Control. Fusion* **46** 233-259

[11]. Gonçalves B, Hidalgo C, Pedrosa MA, Silva C, R Balbín, R, Erents K, Hron M, Loarte A and

Matthews GF, 2003 *Plasma Phys. Control. Fusion* **45** 1627

[12] Pitts R, Fundamenski W, Erents SK, Andrew Y, Loarte, A, Solva C and JET EFDA contributors, 2006 *Nucl. Fusion* **46** 82-98

[13] Evans T.E, Lasnier CJ, Hill DN, Leonard AW, Fenstermacher, ME, Petrie TW, Schaffer MJ, 1995 *J. Nucl. Matter.* **220-222** 235-239

[14] Takahashi H, Fredrickson E.D, Schaffer M.J, Austin M.E, Evans T.E, Lao L.L and Watkins J.G 2004 *Nucl. Fusion* **44** 1075-1096 (2004)

[15] Eich T, Herrmann A and Neuhauser J, 2003 *Phys. Rev. Lett.* **91** 195003.

[16] Endler M, García-Cortés I, Hidalgo C, Matthews GF, ASDEX Team and JET Team 2005 *Plasma Phys. Control. Fusion* **47** 219-240

[17] Kirk A, Eich T, Herrmann A et al, 2005 *Plasma Phys. Control. Fusion* **47** 995-1013

[18] Kirk A, Koch B, Scannell R, Wilson H.R, Counsell G, Dowling J, Herrmann A, Martin R and Walsh M 2006 *Phys. Rev. Lett.* **96**, 185001

[19] Lingertat J, Alper B, Arshad S et al, 22nd EPS Conference on Controlled Fusion and Plasma Physics, Bournemouth, 3rd-7th July 1995, Part 3. p.281.

[20] Clement S, Chankin A, Cirio D, Coad JP, Falter J, Gauthier E, Lingertat J and Puppin S 1999 *J. Nucl. Mater.* **266-269** 285-290

[21] Solano E.R, Villone F, Hawkes N et al, "Current Loss and Strike Point Movement During ELMs in JET", 30th Conf. on Control. Fusion and Plasma Physics, St Petersburg, Russia, July 7–11, 2003, Europhysics Conf. Abs Vol. 26B, 01.106, http://epsppd.epfl.ch/StPetersburg/PDF/P1_106.PDF

[22] Solano E.R, Jachmich S, Villone F, et al, "ELMs and Strike Point Jumps", Proc. of 16th Conf. on Plasma Surface Interactions in Controlled Fusion Devices, Portland Maine, U.S.A, May 24–28, 2004 2005 *J. Nucl. Mater.* **337-339**, 747-750.

[23] Sartori R, Saibene G, Horton LD et al, 2004 *Plasma Phys. Control. Fusio*n **46** 723-750

[24] Herrman A, Neuhauser J, Pautasso G. et al, Proc. of 20th International Atomic Energy Agency (IAEA) Fusion Energy Conference, Nov 2004, Vilamoura, Portugal. IAEA-CN-116/EX/2-4Rb, http://www-naweb.iaea.org/napc/physics/fec/fec2004/datasets/EX_2-4Rb.html

[25] Albanese R, Villone F, 1998 *Nucl. Fusion* **38**, 723- 738

[26] Solano ER, Villone F, "Separatrix instability and ELMs", 31st Conf. on Plasma Physics, London, 28 June-2nd July 2004, Imperial College, London. Europhysics Conf. Abs Vol. 28G, 01.171. http://epsppd.epfl.ch/London/pdf/P1_171.pdf

[27] Saibene G, Lomas PJ, Sartori R et al, 2005 *Nucl. Fusion* **45** 297

[28] Kempenaars M, Beurskens M, de Barr M, 30th EPS Conference on Contr. Fusion and Plasma Phys., St. Petersburg, 7-11 July 2003 ECA Vol. 27A, P-1.56 http://epsppd.epfl.ch/StPetersburg/PDF/P1_056.PDF

[29] ITER Physics Basis, Nucl. Fusion 39 (1999), p.2194

[30] Gill RD, Alper B, Arshad S et al, 1998 *Nucl. Fusion* **38** 1461-1465

[31] Perez CP, Koslowski HR, Huysmans GTA et al, 2004 *Nucl. Fusion* **44** 609-623

[32] Nave MFF, Smeulders P, Hender TC et al, 1997 *Nucl. Fusion* **37** 809-824
[33] Alper B, Dendy RO, Gill RD, Gowers CG, Hender TC, Jones TTC and Contributors to the EFDA-JET Work Programme, Proc. of the 29th EPS Conf. on Plasma Phys. and Contr. Fusion, Montreaux, 17-21 June 2002, ECA Vol. 26 B, P-1.025 (2002) http://epsppd.epfl.ch/Montreux/pdf/P1_025.pdf
[34] Kadomtsev B, 1975 *Sov. J. Plasma Phys*. **1**, 389
[35] Kerner W, Pogutse O P, 1997 *Nucl. Fusion* **37**, 493-499
[36] Evans T E, Moyer RA and Monat P, 2002 *Physics of Plasmas* **9**, 4957-4967
[37] Roeder RKW, Rapoport B I and Evans TE, 2003 *Phys. of Plasmas* **10**, 3796
[38] Cowley SC, Wilson H, Hurricane O, Fong B 2003 *Plasma. Phys. and Contr. Fusion* **45** A31-A38
[39] Kirk A, Wilson HR, Counsell GF, Akers R, Arends E, Cowley SC, Dowling J, Lloyd B, Price M and Walsh M 2004 *Phys. Rev. Lett.* **92** 245002.

Energy(MJ)	$W_{partial}$ before ELM	$W_{partial}/ W_{total}$	$W_{partial}$ after peel at $\Psi = 0.97$	$W_{partial}/ W_{total}$ after peel	Change (MJ)
Pressure:	4.23	1.21%	3.70	1.05%	**-0.53**
Magnetic:					
Plasma					
$B_{poloidal}$	4.13	1.18%	4.08	1.16%	-0.04
$B_{toroidal}$	180.63	51.48%	181.92	51.85%	**+1.30**
Vacuum energy inside vessel					
$B_{poloidal}$	1.51	0.43%	1.49	0.42%	-0.02
$B_{toroidal}$	90.63	25.83%	89.65	25.55%	**-0.98**
Vacuum energy outside vacuum vessel, inside grid					
$B_{poloidal}$	33.36	9.51%	33.22	9.47%	**-0.14**
Iron Core					
$B_{poloidal}$	36.35	10.36%	36.35	10.36%	0
Conductors (poloidal field coils & metal structures with toroidal currents)					
$B_{poloidal}$	56.78	16.18%	56.76	16.18%	-0.02
Total	**350.84**	**100.00%**	**350.42**	**99.88%**	**-0.42**

Table 1. Computed contributions to system energy in model pre-ELM equilibrium for 58837, and with plasma peeled off from Ψ_N=0.97. Contributions from conductor current in the toroidal field coils are not shown, since current in these coils is assumed constant.

Strike point height Z(m)	before ELM		ELM transient		Post-ELM		ΔZ(m)	
	LP	Eq.	LP	Eq.	LP	Eq.	LP	Eq.
Inner strike Z	–1.63	–1.69	–1.40	–1.63	–1.61	–1.65	+.02	+.04
Outer strike Z	–1.64	–1.65	–1.57	–1.57	–1.62	–1.62	+.02	+.03
Filament model	–1.62	–1.66	–1.66	–1.61	–1.61		+.01 to +.05	

Table 2. Z(m) position of strike points, inboard and outboard, comparing LP data and equilibrium reconstruction before ELM, during and after ELM (here Eq corresponds to peeling model described in Section 3), and filament model (in-out symmetric). $\Delta Z = Z_{post\text{-}ELM} - Z_{pre\text{-}ELM}$ .LP spacing is of order 0.02-0.05m, the finest resolution is near –1.63m.

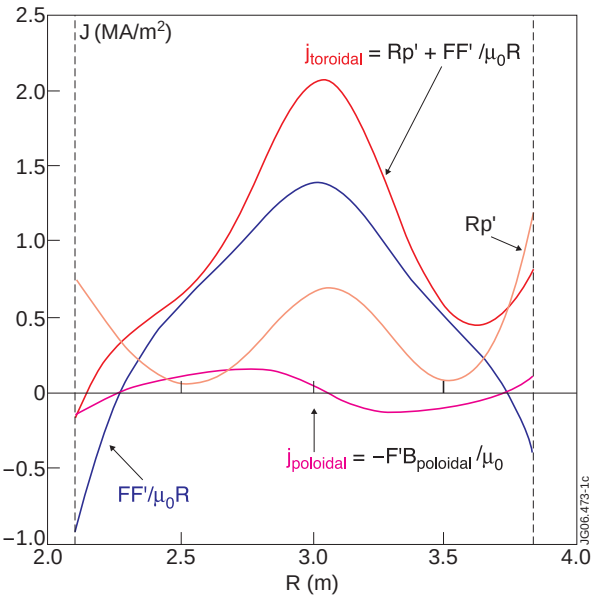

Figure 1: Current densities inside separatrix for JET Pulse No: 58837 at 21.4s, across the plasma equator, just before an ELM. Note the inboard negative toroidal current density due to diamagnetism.

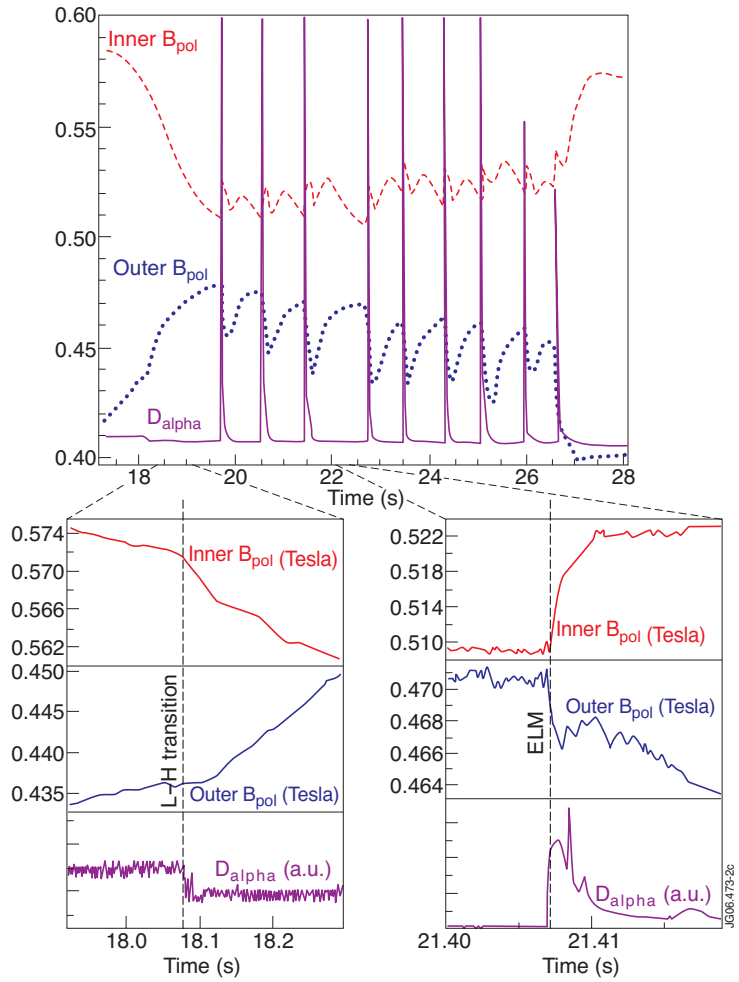

Figure 2: D_α (pink) and local poloidal magnetic fields inboard (red) and outboard (blue). Insets show the L-H transition and one ELM. At the L to H transition, marked by a vertical line, the inner poloidal field decreases (the nearby toroidal current density decreases) and the outer increases (the nearby toroidal current density increases). At the ELM there are opposite variations to the L-to-H transition, indicating that the diamagnetic edge has been lost (see text).

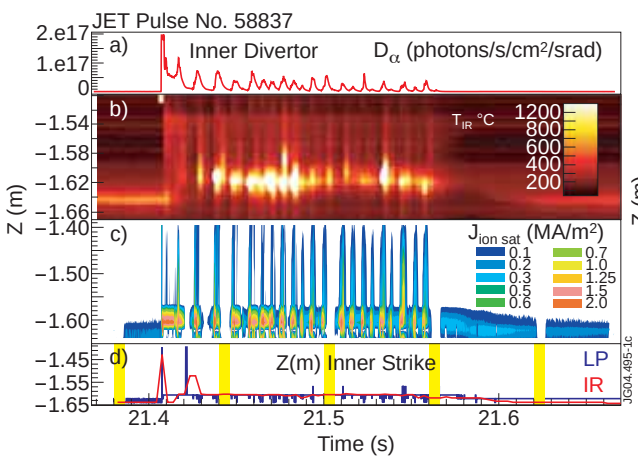

Figure 3: ELM characteristics, at inner divertor leg: a) D_α signal; b) contours of tile temperature T (Celsius) from IR, vs. height at target tile[1]; c) contours of ion saturation current (A/m²), from LPs; vs. probe height along target tile; d) strike position[1,2], as maximum of ion saturation current (LP, blue) and maximum T (IR, red)

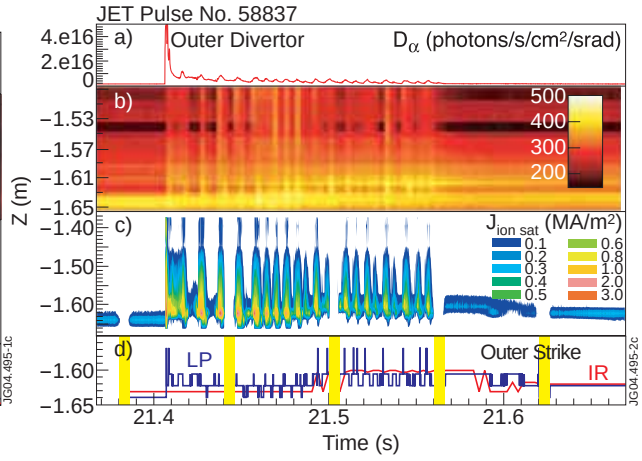

Figure 4: ELM characteristics, at outer divertor leg: same as above[1,2].
[1] Z_{IR} and $time_{IR}$ manually shifted to match Z_{LP} during pre-ELM phase and D_α spike time.
[2] Periodic voltage reversal is applied to LPs to avoid arcs. During this time, marked with yellow bars, strike positions are not well identified by LPs.

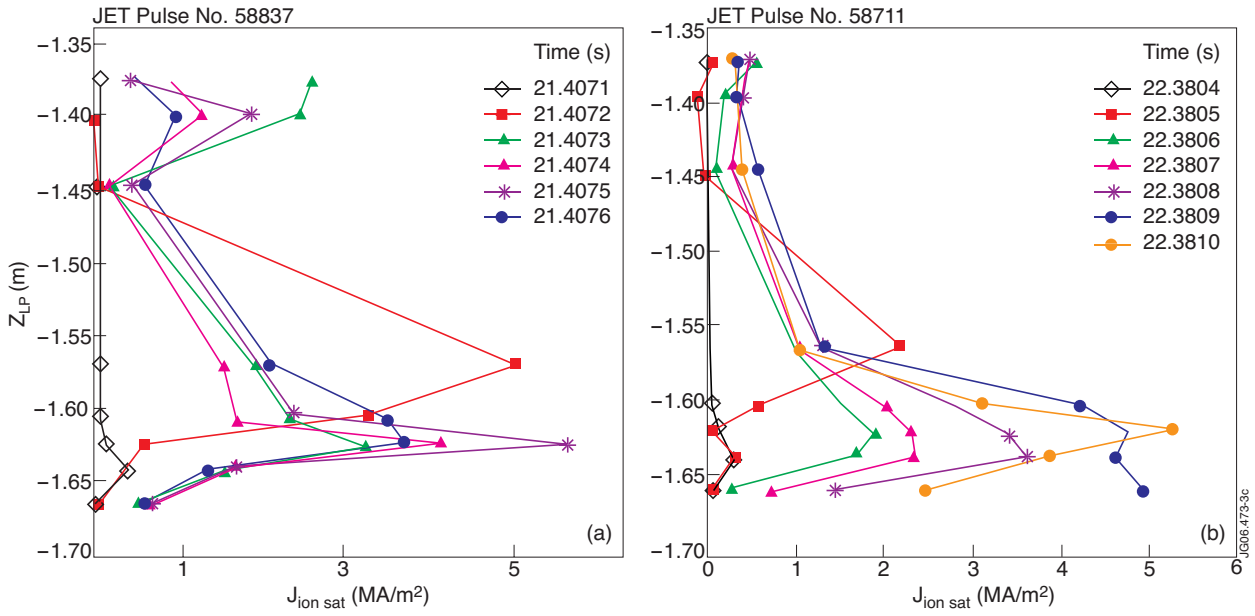

Figure 5: outboard evolution of ion saturation current (horizontal axis) profiles (LP position in vertical axis)
a) Pulse No: 58837: note strike jump in red at 21.4072s, shifted strikes afterwards, possible secondary stripe at the top.
b) Pulse No: 58711: strike jump in red at 22.3805s and shifted strikes afterwards.

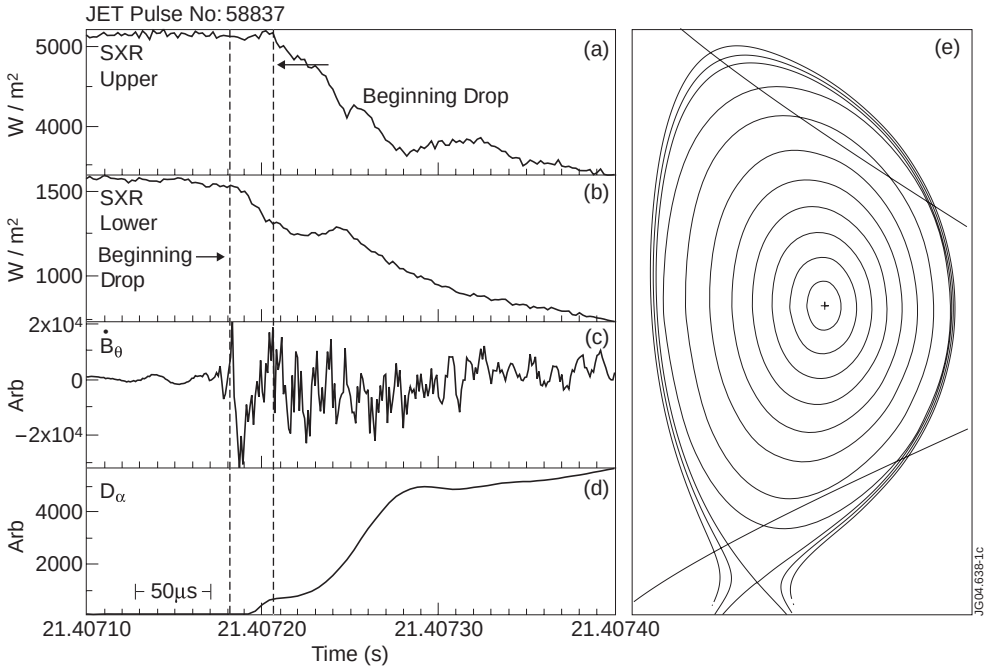

Figure 6: JET Pulse No: 58837 a) SXR amplitude at channel just inside of separatrix at plasma top; b) SXR signal at channel just inside separatrix near X-point (bottom); c)†magnetic fluctuations at inboard coil; d) D_α in inner divertor(e) plasma shape and upper and lower SXR channels shown in (a), (b)

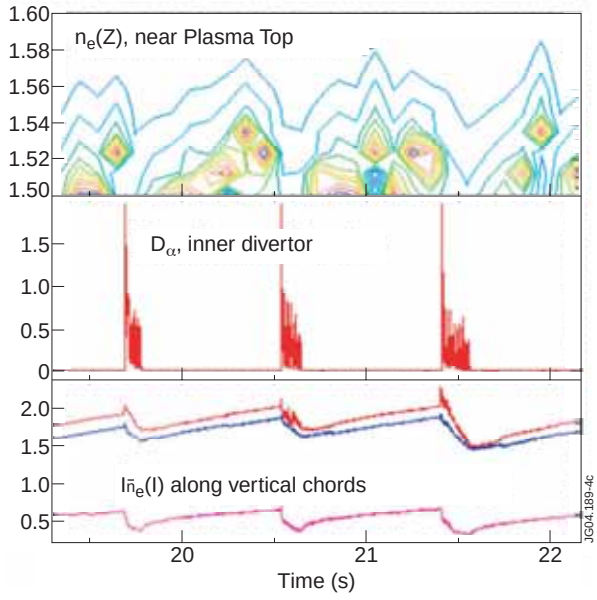

Figure 7: ELM erosion of edge density: a) plasma density contours measured with Li beam at the plasma top; b) D_α in inner divertor; c) line averaged plasma density along 3 vertical chords, 2 central and one at the edge (magenta).

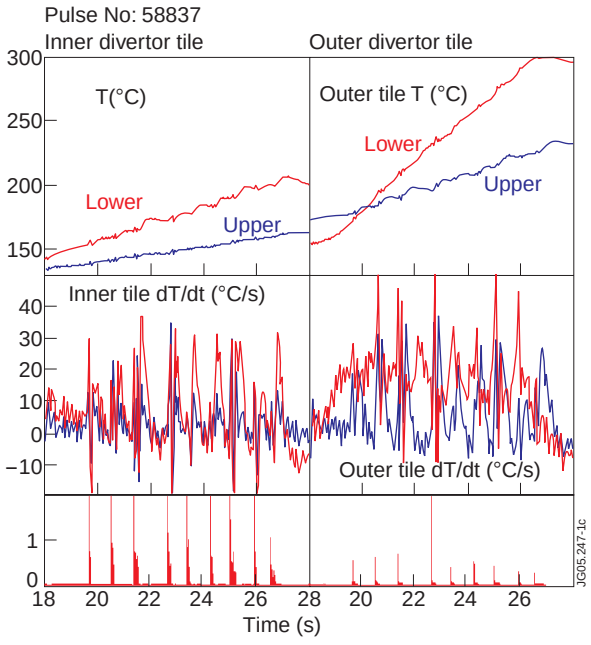

Figure 8: measurements at inner (left) and outer (right) divertor tiles. Top row: temperature in lower and upper TCs. Middle rows: dT/dt (negative spikes at ELM times due to noise pick-up). Bottom rows: D_α signals, showing ELM times.